Calculation of Vibrational Spectra of Linear Tetrapyrroles. 1. Global Sets of Scaling Factors for Force Fields Derived by ab Initio and Density Functional Theory Methods

Ildikó Magdó, Károly Németh, Franz Mark,* Peter Hildebrandt, and Kurt Schaffner

Max-Planck-Institut für Strahlenchemie, Postfach 101365, D-45413 Mülheim an der Ruhr, Germany

Received: July 21, 1998; In Final Form: October 21, 1998

An approach has been developed for calculating the vibrational spectra of linear methine-bridged tetrapyrroles constituting the chromophoric sites of various photoreceptor proteins. Using Pulay's scaling procedure (Pulay, P.; Fogarasi, G.; Pongor, G.; Boggs, J. E.; Vargha, A. *J. Am. Chem. Soc.* **1983**, *105*, 7037), scaling factors were determined for a set of 10 training molecules which mimic structural elements of the tetrapyrrole target molecules. Geometries and force fields were calculated at three theoretical levels, i.e., by the Hartree−Fock (HF), second-order Møller−Plesset perturbation (MP2), and B3LYP density functional theory methods using 6-31G* basis sets. A global optimization yielded sets of 14, 11, and 10 scaling factors for HF, MP2, and B3LYP, respectively. B3LYP provided the best results both with regard to the geometries and the vibrational frequencies. The root-mean-square deviation for the calculated frequencies was 11 cm^{-1} for B3LYP as compared to 13 and 17 cm^{-1} for HF and MP2, respectively. On the basis of the Morse model for an anharmonic oscillator, an expression was derived for correcting scaling factors for the anharmonicity changes in (deuterio) isotopomers. The effects of hydrogen bonding interactions via N−H···O═C bonds on the structures and vibrational spectra were studied in the case of maleimide. For the N−H stretching, deformation, and out-of-plane wagging vibrations, modifications of the scaling factors are required in order to reproduce the vibrational spectra of the hydrogen bonded dimer. The IR and Raman intensities calculated by the B3LYP method were found to agree well with experimental spectra. For the Raman intensities, a fourth-order differentiation formula was derived for the numerically accurate calculation of polarizability derivatives with respect to Cartesian displacements, by using the finite field method.

Introduction

Linear methine-bridged tetrapyrroles constitute an important class of prosthetic groups in protein systems with quite different biophysical functions due to the structural flexibility of these chromophores.[1] In photosynthetic antenna pigments linear tetrapyrroles are organized in the protein matrix in a way which allows for a highly efficient energy transfer to the reaction centers.[2] While these processes require a well defined and fixed chromophore structure, the function of the photoreceptor phytochrome, which is involved in steering photomorphogenic processes, is intimately associated with extended structural changes of the protein-bound tetrapyrrole (Figure 1).[3] This 124-kDa chromoprotein utilizes light as a source of information inasmuch as a photoinduced reaction cycle of the protein eventually leads to the conversion of the inactive (P_r) to the active form (P_{fr}) of phytochrome capable of triggering a physiological reaction cascade. Evidently, the elucidation of the structural changes of the chromophore during the reaction cycle is a prerequisite for understanding the mechanism of activation of phytochrome.

Even for the stable states P_r and P_{fr}, however, the structure determination by X-ray crystallography and NMR spectroscopy is not (yet) possible due to the lack of adequate crystals or due to the protein size. Therefore, other spectroscopic techniques have to be employed. Among these, resonance Raman (RR) spectroscopy represents the most promising approach since it selectively probes the vibrational band pattern of the chromophore upon excitation in resonance with its electronic transition.[4] Moreover, this technique is appropriate also to study intermediates. In fact, high quality RR spectra have been obtained from the parent states P_r and P_{fr} as well as from several intermediates formed during the reaction cycle.[5]

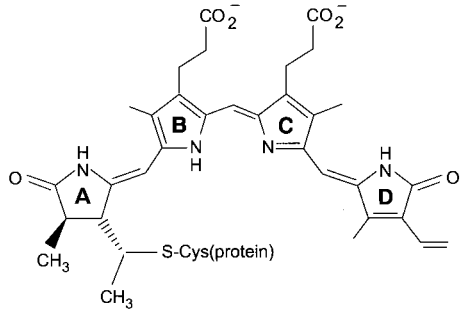

Figure 1. Structural formula of the protein-bound phytochromobilin chromophore.

These RR spectra include detailed information about the configuration and conformation of the protein-bound tetrapyrrole and its interactions with the immediate protein environment. Moreover, RR spectra can reflect even subtle structural differences of the active sites in chromoproteins which are beyond the resolution of X-ray data. With regard to the information content, vibrational spectroscopies can thus well compete with diffraction techniques and NMR spectroscopy. However, the current state of extracting this information from the spectra is by far more advanced in the latter methods. Hence, decoding of the RR spectra of phytochrome is not only a prerequisite for

* Corresponding author.

10.1021/jp983101g CCC: $18.00
Published on Web 01/14/1999

the elucidation of structure−function relations in this protein, but it is also a challenge since a general strategy is needed for the analysis of the vibrational spectra of large, highly substituted and nonsymmetric molecules such as linear tetrapyrroles.

In principle, there are two approaches to tackle this problem. Empirical force fields have been employed for the normal-mode analysis of cyclic tetrapyrroles, i.e., porphyrins.[6,7] The high symmetry of this class of compounds and the large body of experimental data, including spectra of numerous isotopomers, significantly facilitate the vibrational assignments. However, these advantages do not exist for linear tetrapyrroles so that an empirical approach has been attempted so far only for the pyrromethenone fragments of bilirubin.[8] Calculations of the force fields by quantum chemical methods are clearly a viable alternative for linear tetrapyrroles.

For large molecules which are comparable in size to linear tetrapyrroles semiempirical approaches were the only applicable methods for a long time.[9] However, the rapid progress of computational facilities as well as the availability of efficient software now opens the possibility to apply more demanding computational methods to such molecules.[10−12]

The crucial problem of quantum chemical force field calculation, both in semiempirical and ab initio methods, is to account for errors which result from deficiencies of the quantum mechanical method and from the harmonic approximation.[13] These errors can be partially corrected by scaling procedures. While scaling of the calculated frequencies by a single factor already significantly improves the agreement with experimental frequencies,[14] a physically substantiated method, pioneered by Pulay and co-workers, is based on scaling of the force field itself.[15] The underlying idea is that the intrinsic error of force constants is systematic and specific for the internal coordinates involved so that the corresponding scaling factors should be the same whether the force constants refer to the same or to quite similar internal coordinates. This model implies that scaling factors are transferable between different molecules that include similar internal coordinates. Consequently, these scaling factors can be determined for molecules for which a complete vibrational assignment is straightforward, and they can then be transferred to the target molecules.

Our first attempts of a vibrational analysis of a linear tetrapyrrole, biliverdin dimethyl ester IX (BVE) (Figure 2), were guided by this concept.[16] We had chosen this compound as a target molecule in view of its similar constitution with respect to phytochromobilin, the tetrapyrrole chromophore of phytochrome. It is one of the few linear tetrapyrroles for which a crystal structure has been determined.[17] In addition, specifically deuterated isotopomers of BVE can be synthesized and configurational isomers can be prepared which is of particular importance for extending the experimental data set.[18] In the BVE study,[16] we have employed the semiempirical AM1 method to calculate the force field. Preliminary scaling factors were obtained from the vibrational analysis of a set of small molecules representing BVE "fragments" (pyrrole, maleimide, ethene, and acetic acid). Calculated RR and IR intensities afforded additional criteria for plausible assignments of the observed bands which, up to now, only in a few cases had to be revised in view of more recent experimental data of BVE isotopomers.[18] Despite the first encouraging results, the limitations of this study became evident, partly because the number of "fragment" molecules was relatively small. Moreover, it is meanwhile well established that the errors in semiempirical calculations are far less systematic than in ab initio calculations,[19] casting some doubt on the transferability of scaling factors within the AM1

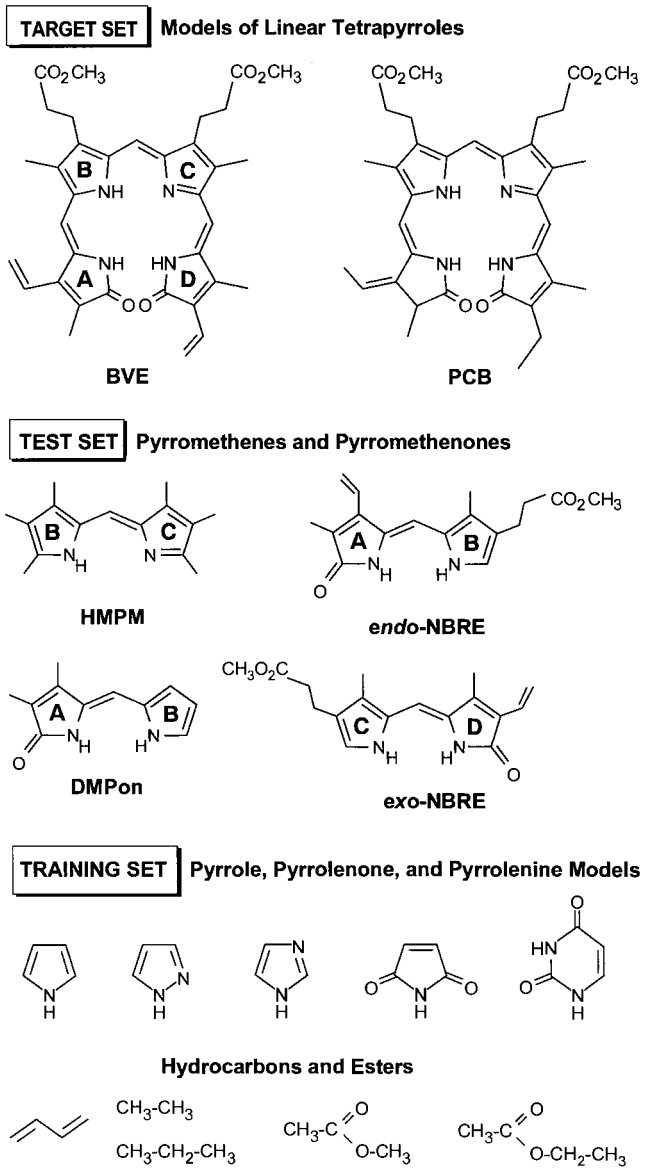

Figure 2. Structural formulas of the target, test, and training molecules.

approach. Finally, intermolecular interactions, i.e., hydrogen bonding interactions, have not been considered although these are known to be relevant both in solutions and in the crystal.[20,21]

In an attempt to overcome these limitations, we have now developed an approach including several conceptional and methodological improvements. First, the force fields were calculated at the ab initio Hartree−Fock (HF) and density functional theory (DFT) levels. Among the various density functional forms proposed we have chosen Becke's three-parameter hybrid functional (B3LYP)[22] which yields both excellent geometries and vibrational frequencies for compounds containing first row elements.[23−28] In particular, Rauhut and Pulay[29] have shown that errors of vibrational frequencies obtained with B3LYP are also systematic and, hence, can be corrected by appropriate scaling procedures. Besides the HF and B3LYP methods, we have also employed the second-order Møller−Plesset perturbation approach (MP2) with frozen core orbitals even though we did not intend to apply this method to our target molecules due to the high requirements for computational time and disk storage. Second, following Rauhut and Pulay,[29] we have established a set of scaling factors by globally fitting to the vibrational spectra of 10 small molecules, i.e., the training set, which represent the structural motifs of methine-

bridged tetra-(oligo-)pyrroles. Using this "global" fit procedure the probability of running into local minima and to obtain artifacts is largely reduced. Third, IR and Raman intensities were calculated to support the vibrational assignment. Fourth, hydrogen-bonding interactions were considered for selected training set molecules, and scaling factors were derived for the NH group in hydrogen-bonded systems.

This approach results in a global set of scaling factors which—as will be shown in subsequent publications[30]—is appropriate to predict accurately the IR and Raman spectra of various dipyrroles (test molecules). For their hydrogen-bonded dimers modifications of the scaling factors are only required for the NH groups involved in hydrogen bonding. The approach therefore promises to describe the vibrational spectra of BVE and other tetrapyrroles (target molecules) as well.

The present paper is divided into four sections. At first, we discuss our choice of training molecules which are regarded to be appropriate for determining a global set of scaling factors for the target molecules (section I). The results of the geometry optimization for the individual training molecules in comparison with experimental data are summarized in section II. Subsequently, we present the results of the force field scaling and the construction of a global set of scaling factors (section III). Finally, we outline the determination of the IR and Raman intensities (section IV).

In this paper, emphasis is laid on the generalization of the results obtained from the individual compounds while details of their vibrational analysis and the underlying quantum chemical calculations will be published elsewhere.[30a]

Methods

All quantum mechanical calculations were carried out on a Dec Alpha workstation AS 600 5/333 using the program package GAUSSIAN94.[31] Programs developed in our laboratory were employed for the normal-mode analysis as well as for the determination of the scaling factors and the evaluation of the B3LYP Raman intensities.

Geometries were optimized with the TIGHT option of the GAUSSIAN94 program. The FINE GRID option was used for the numerical integrations. With finer grids (or larger spherical grids) an improvement was achieved only for the six zero-frequency modes while the normal-mode frequencies were not affected considerably. On the other hand, such grids lead to a significant increase of the computational time, which would be a serious obstacle for extending the calculations to larger molecules.

In preliminary calculations of selected training molecules we have compared various basis sets. Using 6-31G basis sets without polarization functions, distinct deviations of the calculated geometries from the experimental data were found. For instance, the pyramidalization angle of the lactame unit in pyrrolidone (a model for ring A in phytochromobilin, see Figure 1) was calculated too low by all three methods (2.4−3.4°), whereas the 6-31G* basis provided a substantially better agreement (9.4−11.6°) with the experimental data (12.1°).[32] No further improvements were achieved with the 6-31G** basis (8.8−11.4°), the considerably larger computational efforts of which were therefore not justified. Furthermore, deficiencies noted for hydrogen-bonded systems—as will be discussed below—could not be removed even with this basis set. Thus, the 6-31G* basis was employed for all calculations used to construct global sets of scaling factors. The results obtained with this basis set will be referred to by the short-hand notations HF, B3LYP, and MP2.

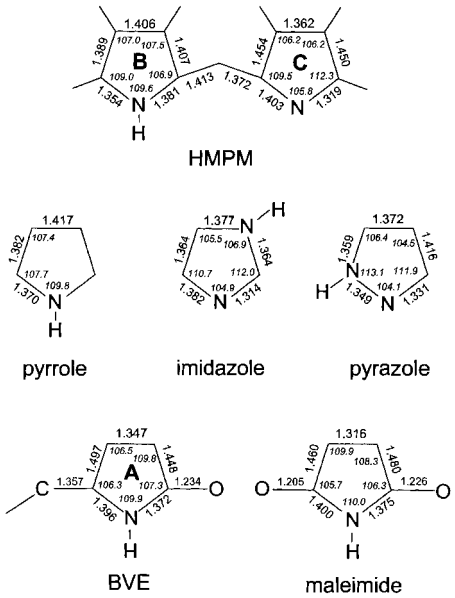

Figure 3. Experimental structures of ring A of BVE[17] and of HMPM[30b] in comparison with those of various heterocycles.[34−37]

I. Target, Test, and Training Molecules. The hierarchy of the molecules constituting the benchmarks of the project is illustrated in Figures 1 and 2. The *target molecules* do not only include BVE as a model for phytochromobilin but also phycocyanobilin (PCB) which differs from BVE in ring A (chiral carbon and *exo*-ethylidenic group instead of an endocyclic double bond) and in the substitution pattern of ring D (ethyl vs vinyl). PCB is of considerable value as a model for the protein-bound tetrapyrrole in phytochrome since in contrast to biliverdin, it has been successfully used in reconstitution experiments with phytochrome apoprotein resulting in structural, photochemical, and kinetic properties very similar to those of the native holoprotein.[33]

The set of *test molecules* comprised four methine-bridged dipyrroles. This set is to be used to check the reliability of the approach and the quality of the global scaling factors. The test compounds represent building blocks of the target molecules (Figures 1 and 2). While *endo*-neoxanthobilirubinic ester (*endo*-NBRE) and 3,4-dimethylpyrromethenone (DMPon) mimic the A−B dipyrrole unit of the tetrapyrrole, *exo*-NBRE includes the C−D dipyrrole unit except for the pyrrolenine structural motif (ring C). The latter, however, is represented by hexamethylpyrromethene (HMPM), a model for the B−C unit.

The *training molecules* serve for the determination of scaling factors which are transferable to the test and target molecules. Hence, the principal criterion for choosing the training molecules is that they include the same or similar internal coordinates as the target molecules. This does not necessarily imply that the chemical constitution of such a molecule must be fully contained in the target molecules. However, essential structural elements must be the same or, at least, very similar. A second criterion is the availability of accurate structural data for a performance check of the quantum mechanical geometry calculation. Finally, experimental IR and Raman spectra of the compounds in well-defined states (preferentially monomeric states) are needed since the determination of the scaling factors requires a safe vibrational assignment. In this way, we have selected a series of 10 different compounds (Figure 2) which together with the deuterated isotopomers constitute 13 sets of vibrational frequencies.

Heterocyclic Compounds. The only pyrrole-derived ring among the target molecules is ring B which in the tetrapyrroles

TABLE 1: Mean Deviations of Calculated Bond Lengths (in angstroms) from the Experimental Values[a]

	HF		MP2		B3LYP	
	X−Y	X−H	X−Y	X−H	X−Y	X−H
pyrrole[35]	0.016	0.006	0.002	0.008	0.006	0.007
imidazole[36]	0.015	0.008	0.008	0.007	0.004	0.007
pyrazole[37]	0.018	0.007	0.011	0.008	0.004	0.006
maleimide[42]	0.021		0.012		0.008	
uracil[43]	0.019		0.011		0.008	
methyl acetate[44,45]	0.022		0.009		0.010	
ethyl acetate[38]	0.018		0.016		0.014	
butadiene[46]	0.016	0.016	0.003	0.006	0.003	0.006
ethane[47]	0.005	0.010	0.006	0.003	0.001	0.000
propane[40]	0.002	0.007	0.000	0.003	0.006	0.004
average	0.016	0.010	0.008	0.006	0.006	0.006

[a] Abbreviations: X and Y refer to C, N, or O atoms. Experimental data were taken from the literature.

possesses an asymmetric substitution pattern including two unsaturated side chains. Model compounds which would mimic such a conjugated pyrrole are not stable. The effect of conjugated substituents on the pyrrole geometry can readily be seen by comparing the bond length patterns in pyrrole and HMPM (Figure 3). These experimental trends should be reproducible by the quantum mechanical calculations and, therefore, should not require specific training molecules. Indeed, the structure of HMPM calculated at the B3LYP level is in very good agreement with that determined by X-ray analysis.[30b]

The choice of an appropriate model for the pyrrolenine ring C is not straightforward. We have chosen pyrazole and imidazole which can be considered as imino-substituted pyrrolenines (Figure 3). Although in both compounds the bond length alternation is less pronounced than in ring C, a similar pattern of bond lengths and bond angles suggests nevertheless that these compounds are satisfactory models. Since pyrazole and imidazole may be viewed, alternatively, as aza-substituted pyrroles, they also serve as models for ring B.

Training set molecules which are closely related to the rings A and D are lactams for which we have chosen maleimide and uracil. In fact, the available structural data (Figure 3) reveal striking similarities between maleimide and BVE which both form hydrogen-bonded dimers in the solid state.[17,34] The six-membered ring of uracil is of particular interest as it does not only include the lactam unit but also an additional conjugated amide motif reminiscent of the C−N bond adjacent to the methine bridge in BVE (DMPon, *endo*-NBRE, and *exo*-NBRE).

Hydrocarbons and Esters. Ethane and propane include essentially all internal coordinates which are involved in the methyl, ethyl, and propionate side-chains. Two compounds were used to mimic the propionic ester group. Besides methyl acetate as a model for the acetoxy group we included ethyl acetate as a structural isomer of methyl propionate in order to increase the data set. Butadiene is taken as a model not only for the methine bridges but also for the vinyl substituents in BVE. In contrast to ethene which was chosen in our previous study,[16] the open-chain conjugated system of butadiene may more closely model the conjugated methine bridges and vinyl groups of the target molecules.

II. Geometry Calculations. To assess the performance of the quantum mechanical methods, the structures calculated for the training molecules at the HF, MP2, and B3LYP levels were compared with experimental data. In general, gas phase structural data were used for comparison except for ethyl acetate for which only X-ray crystal data have been reported.[38] Preferably, r_s structures were used which are close to the r_e structures obtained by quantum chemical calculations.[39] These geometries are available for pyrrole,[35] imidazole,[36] pyrazole,[37] and propane.[40] Otherwise, r^0_α and r_z structures, which were obtained by electron diffraction and spectroscopic methods, respectively, were employed. These structures are corrected for vibrational motion and extrapolated to 0 K. The mean deviations[41] between calculated and experimental X−Y and X−H bond lengths are compiled in Table 1.

Heterocycles. Pyrrole, imidazole, and pyrazole provide a unique subset of training molecules since the r_s structures have been determined for all of them. The calculations yield planar ring structures which are in line with the experimental findings.

For the bond lengths of the heavy-atom skeleton, B3LYP calculations yield an excellent description with only small deviations from the experimental values. There is a subtle overestimation of the C═C bonds in pyrazole and imidazole ($\Delta R \approx +0.008$ Å) but not in pyrrole ($\Delta R = -0.004$ Å), ruling out the hypothesis that these deviations reflect a general tendency. For the single bonds, the deviations are smaller and do not show a systematic pattern. Good results are also obtained with MP2, although the average errors for the heterocycles are somewhat larger than with B3LYP (0.008 Å vs 0.005 Å). The larger deviations are mainly due to an overestimation of the C═C and C═N lengths in pyrazole and imidazole. Pyrrole constitutes an exception inasmuch as MP2 yields a striking agreement ($\Delta R = 0.002$ Å) as already found by Simandiras et al.[48] The results obtained at the HF level are clearly worse as all calculated bond lengths (except for the $C_\beta-C_{\beta'}$ bond in pyrrole) are too long. In particular, the double bonds deviate on the average by as much as 0.022 Å.

B3LYP provides the best results also for the bond lengths involving the hydrogen atoms, although HF and MP2 perform almost equally well. There is a systematic overestimation of the bond lengths at the B3LYP and MP2 levels, in particular of the N−H bonds by 0.012 and 0.014 Å, respectively, whereas HF underestimates N−H and C−H bond lengths.

With regard to the calculated bond angles, again the best results are obtained with B3LYP (mean deviation 0.3°), while the quality of the MP2 and HF results is slightly inferior (0.4° in both cases).

Lactams. For maleimide[42] and uracil,[43] the deviations for both bond lengths and bond angles are larger than for the heterocyclic compounds. For the present comparison, we only considered the geometry of the heavy-atom frame since the relative positions of the hydrogens were not determined directly in the electron diffraction studies. The main contribution to the average bond length deviations is associated with the C−N single bonds adjacent to the C═C double bonds. For each method, the calculated length of this C−N bond is too small. Systematic discrepancies between predicted and experimental values are also be observed for some bond angles. The mean deviations

for bond angles are 1.9° and 1.5° for maleimide and uracil, respectively, and they are about the same for all three methods. These large deviations are mainly due to the contributions from specific angles such as the N−C═O angle in maleimide and several ring angles in uracil, for which experimental and theoretical values differ by about 2−3°.

Esters and Hydrocarbons. For methyl acetate, gas-phase structural data are available. However, there are notable discrepancies between the structures reported. The electron diffraction study by O'Gorman et al.[44] yielded a C(sp^3)−O bond length of 1.46 Å which was noted to be unusually long. In fact, it is not reproduced by the calculations. More recently, Pyckhout et al.,[45] who combined electron diffraction and calculated HF/4-21G data in the structure analysis, reported a shorter bond length. With respect to these results, the mean deviations of the present calculations are generally smaller. In this particular case, they are somewhat higher for B3LYP than for MP2 (Table 1), although this is due solely to a 0.019 Å deviation for the C(sp^3)−C(sp^2) bond length. For this specific bond, an inconsistency has already been noted by Pyckhout et al.[45] with regard to the empirical correction needed to convert the r_g into the r_α^o structure.

For ethyl acetate, only X-ray structural data are available for crystals in which the ester is included as a solvate.[38] Hence, the underlying intermolecular interactions and their effect on the ester structure may be the main reason for the substantial deviations of the calculated bond lengths reflected by average values of 0.014, 0.016, and 0.018 Å for B3LYP, MP2, and HF, respectively. In particular, the calculated C(sp^2)−O single bond length is too long at the B3LYP and MP2 levels as compared to the experimental value. This discrepancy is in contrast to methyl acetate for which the calculated value of this bond length agrees very well with the gas phase structure.

Butadiene[46] appears to be an instructive example for the deficiencies of the HF approach as compared to MP2 or B3LYP. While the latter two methods provide an excellent agreement with the experimentally determined bond lengths (C═C, C−C, C−H), HF overestimates the C−C and C═C bond length alternation. Hence, the overall agreement of the HF calculations is much better for the saturated hydrocarbons, but still beyond the quality of the MP2 and B3LYP results.

Overall Comparison of the Computational Methods. The comparison of the data in Table 1 demonstrates that inclusion of electron correlation effects, at either the MP2 or the B3LYP level, significantly improves the quality of the results. Compared to the HF approximation, the deviations are reduced by a factor of 2−3. The performance of the B3LYP method is somewhat better than that of the MP2 method. This is particularly true for the heterocyclic compounds with well determined structures where the B3LYP results are close to the experimental accuracy. Indeed, it has been shown by Martin et al.[24] that geometries calculated by using the B3LYP functional and a basis comparable to the 6-31G* set may be even more accurate than those obtained from highly correlated coupled cluster calculations with larger basis sets, due to an error compensation. In general, the ranking of the theoretical methods is in line with that from previous comparative studies of organic compounds containing first-row elements.[23−28]

III. Scaling of the Force Fields. A crucial step in determining the scaling factors is the choice of the experimental data set. We critically considered available experimental data by taking into account the specific experimental conditions and the accuracy of the measurements as well as the calculated data (frequencies, band intensities, and mode compositions) obtained in this work and reported in the literature. The availability of gas phase or matrix IR (Raman) data and a reliable vibrational assignment were essential criteria for the selection of training molecules. It should be mentioned that the quality of the fits of the scaling factors per se did not provide an additional criterion for the assignment. This is particularly true for ambiguities associated with closely spaced modes. In such cases, equally good fits were obtained with either assignment since the individual scaling factors did not differ strongly from each other. Nevertheless, we did not omit any modes from the fitting procedure even if the calculated frequencies revealed substantially larger deviations from the experimental values as compared to the average deviation. A total of 301 experimental frequencies was finally included in the least-squares procedure. The detailed vibrational analyses of the various training set molecules are discussed elsewhere.[30a]

Scaling of the calculated force fields followed the general procedure introduced by Pulay and co-workers.[15] The scaled force constants $(F_{ij})^\sigma$, which refer to internal coordinates i and j as defined by Pulay et al.,[49] are obtained according to eq 1,

$$(F_{ij})^\sigma = \sqrt{\sigma_i}(F_{ij})\sqrt{\sigma_j} \qquad (1)$$

where F_{ij} are the calculated (unscaled) force constants and σ_i and σ_j are the scaling factors. The total number and the kind of scaling factors were selected in an iterative way for each of the three methods. As shown recently by Rauhut and Pulay,[29] the scaling factors in DFT calculations for several diagonal force constants tend to assume the same values. For instance, for organic compounds involving the first-row heavy atoms X, Y, and Z, i.e., C, N, O, the X−Y bond stretching and the XYZ bond angle deformation force constants required only one scaling factor each. Thus, the scaling factors are well transferable and their number can be kept small. In the present study, the reduced parameter set of Rauhut and Pulay[29] served as a guideline for the construction of the initial sets. During the fitting process this parameter set was further modified either by separating into different scaling factors in order to reduce systematic deviations or by additional grouping of scaling factors. The final results are listed in Table 2.

The values of the scaling factors in MP2 and B3LYP are much closer to unity than those in HF. This well-known tendency reflects the intrinsic consideration of electron correlation effects by these methods, which leads to a substantial lowering of the systematic errors of force constant calculations. Note that the B3LYP scaling factors display a much smaller deviation from unity than the MP2 values. The number of different scaling factors is reduced from 14 in HF to 11 and 10 in MP2 and B3LYP, respectively. Whereas at the B3LYP level single and double bond stretching force constants between heavy atoms can be scaled by the same factor, the HF and MP2 force constants require two different scaling factors. This is also true for the C−H and N−H stretching force constants. The MP2 method, however, is superior with regard to the scaling of the out-of-plane (oop) vibrations (one factor), since two and three different factors are required in B3LYP and HF, respectively.

In general, the values of our B3LYP scaling factors agree well (within less than 1%) with those obtained by Rauhut and Pulay.[29] However, for the torsional and the NH deformation (NH def) force constants there are larger discrepancies, with 9.6%, 3.3%, and 12.3% deviations for the NH deformation, single bond torsion, and conjugated bond torsion, respectively. One should note that Rauhut and Pulay[29] employed only a single scaling factor for all oop vibrations whereas our set of training molecules required an additional scaling factor for the NH oop

TABLE 2: Globally Optimized Scaling Factors for the Set of Training Molecules[a]

B3LYP		HF		MP2	
internal coordinate	σ_i[b]	internal coordinate	σ_i	internal coordinate	σ_i
X−Y, X═Y str	0.9242 (0.0009)	X−Y str	0.8387	X−Y str	0.8860
C(N)H str	0.9153 (0.0003)	CH str	0.8259	CH str	0.8815
XYZ angle def	0.9960 (0.0023)	XYZ angle def	0.8343	XYZ angle def	0.9894
HCH def	0.9168 (0.0009)	HCH def	0.7861	HCH def	0.8771
XCH def	0.9498 (0.0012)	XCH def	0.8097	XCH def	0.9145
oop (not NH)	0.9870 (0.0015)	oop (not NH, C═O)	0.7428	oop	1.0654
single bond torsion	0.9668 (0.0112)	single bond torsion	0.8520	single bond torsion	0.8488
conj bond torsion	0.9482 (0.0026)	conj bond torsion	0.8120	conj bond torsion	0.9755
NH def	0.9693 (0.0038)	NH def	0.7624	NH def	0.9579
NH oop	1.0120 (0.0051)	NH oop	0.8828		
		X═Y str	0.7427	X═Y str	0.9219
		NH str	0.8024	NH str	0.9110
		C═O oop	0.8077		
		C−O ester str	0.7314		

[a] Abbreviations: X, Y, and Z refer to C, N, or O atoms; str, stretch; def, deformation; oop, out-of-plane; conj, conjugated. [b] Standard deviations are given in parentheses.

vibration. We found, furthermore, that a specific NH def scaling factor improved the global fit.

In a least-squares treatment, the standard deviations of the optimized parameters are an approximate measure of the uncertainty in each parameter. These values are shown in Table 2 for the B3LYP scaling factors. In general, the standard deviations are small indicating that our data set of experimental frequencies was sufficiently large to determine the scaling factors reliably. A greater uncertainty, however, is noted for the single bond torsion suggesting that a single scaling factor for single and double bond torsion might be applicable as well. Despite the fact that for this 9-parameter set the rms deviation of the global fit is only slightly increased, we preferred the 10-parameter set to provide a more flexible parametrization for ring A of tetrapyrroles which may either be fully conjugated or partially unsaturated (Figures 1 and 2).

An ambiguity is associated with the assignment of some internal coordinates to specific scaling factors when using the definitions by Pulay et al.[49] For instance, in the internal coordinates of CH_2 and CXY scissoring, the HCH def and XCH def vibrations are mixed with different weights in each coordinate. In these cases, we assigned the HCH def (XCH def) scaling factor to the coordinate with the largest weighting factor for the HCH def (XCH def) vibration. The small standard deviations for these scaling factors indicate that only a marginal error is introduced by this approximation. A rigorous treatment would require a transformation from Cartesian to internal coordinates using a transformation matrix which depends on the scaling factors. Furthermore, the formulas for the analytic derivatives of the frequencies with respect to the scaling factors required for parameter optimization[50] would have to be generalized. It should be mentioned that recently a procedure has been presented for the direct scaling of primitive valence force constants.[51]

Anharmonicities and Deuterated Isotopomers. For some of the training molecules, also deuterated isotopomers were included in the determination of the scaling factors. Therefore, it had to be taken into account that the scaling factors σ_i correct for both anharmonic effects and deficiencies of the quantum chemical method. Assuming that these corrections are independent of each other, σ_i may be written as a product of two factors, i.e.,

$$\sigma_i = (\sigma_i)^q(\sigma_i)^a \tag{2}$$

where the superscripts q and a refer to the quantum chemical and the anharmonic corrections, respectively. On the basis of the Morse oscillator model a correction factor $(\sigma_{XD})^c$ for the X−D stretching coordinate is derived in Appendix I which is given by eq 3,

$$(\sigma_{XD})^c = \left(\frac{1 - 2x_{e,XH}\sqrt{\frac{\mu_{XH}}{\mu_{XD}}}}{1 - 2x_{e,XH}}\right)^2 \tag{3}$$

where μ_{XH} and μ_{XD} are reduced masses and $x_{e,XH}$ relates the anharmonic frequency ν_{XH} of the Morse oscillator to the harmonic frequency $\omega_{e,XH}$ according to eq 4,

$$\nu_{XH} = \omega_{e,XH}(1 - 2x_{e,XH}) \tag{4}$$

Multiplying $(\sigma_{XD})^c$ with the scaling factor σ_{XH} as obtained by the fitting procedure for the nondeuterated species, one readily determines the scaled force constant $(F_{XD})^\sigma$ which holds for the deuterated isotopomers according to eq 5,

$$(F_{XD})^\sigma = \sigma_{XH}(\sigma_{XD})^c F_{XH} \tag{5}$$

According to eq 3, anharmonicity effects are particularly pronounced for deuteration whereas those due to substitutions by other isotopes, e. g., ^{13}C and ^{15}N, can be neglected. Moreover, the anharmonicity is relatively high for X−H stretchings and hence, corrections for X−D stretchings are not negligible. Such effects are much less pronounced, for instance, for X−H/X−D deformations. Also, some oop deformation and torsional modes

TABLE 3: X−H Stretching Modes (in cm^{-1}) of Pyrrole and Deuterated Isotopomers[a]

		A_1			B_1	
symmetry		$\nu_{NH(ND)}$	$\nu_{CH(CD)}$	$\nu_{CH(CD)}$	$\nu_{CH(CD)}$	$\nu_{CH(CD)}$
pyrrole	exptl	3527	3148	3125	3140	3116
	B3LYP	3513	3144	3123	3139	3111
	difference	−14	−4	−2	−1	−5
pyrrole−ND	exptl	2606	3148	3126	3142	3115
	B3LYP	2607	3144	3123	3139	3111
	difference	1 (−2)	−4 (−4)	−3 (−3)	−3 (−3)	−4 (−4)
pyrrole-D4	exptl	3531	2375		2340	2305
	B3LYP	3513	2368	2333	2357	2320
	difference	−18 (−18)	−7 (−29)		17 (6)	15 (−8)
pyrrole-D5	exptl	2607	2376	2325	2347	2305
	B3LYP	2608	2368	2333	2356	2320
	difference	1 (−26)	−8 (−31)	8 (−14)	9 (−13)	15 (−8)

[a] The experimental data were taken from ref 56. Calculated frequencies for the deuterated isotopomers were obtained after anharmonicity correction (differences between the experimental values and those calculated without anharmonicity correction are given in parentheses).

TABLE 4: NH Stretching, Deformation, and Out-Of-Plane Modes (in cm^{-1}) for Various Training Set Molecules[a]

	NH stretching			NH deformation[b]			NH out-of-plane		
	exptl	calcd	difference	exptl	calcd	difference	exptl	calcd	difference
pyrrole[57]	3531	3513	−18	1424	1435	11	475	450	−25
				1134	1139	5			
pyrrole-ND[56]	2606	2607	1	906	914	8	372	354	−18
		(2580)	(−26)	827	836	9			
pyrazole[58]	3523	3509	−15	1531	1537	6	516	499	−17
				1447	1459	12			
pyrazole-ND[58]	2640[c]	2606		955	960	5	406	398	−8
		(2579)		858	871	13			
imidazole[59]	3517	3494	−23	1407	1413	6	509	504	−5
				1085	1074	−11			
maleimide[60,61]	3482	3492	10	1346	1328	−18	504	521	17
				1285	1295	−10			
maleimide-ND[61,62]	2600	2592	−8	1218	1191	−26	375	385	10
		(2565)	(−35)	797	794	−3			
uracil[63]	3484	3483	−1	1472	1473	1	660	688	28
	3435	3448	13	1389	1383	−6	551	564	13
uracil-1,3-D[64,d]	2593	2582	−11	918	917	−1	501	525	24
		(2555)	(−38)	821	813	−8	420	428	8
	2549	2555	6						
		(2528)	(−21)						

[a] Calculated frequencies were obtained by B3LYP; values without anharmonicity correction are given in parentheses. [b] Only the two modes with the largest NH deformation contribution are listed. [c] Perturbed by Fermi resonance (see ref 65). [d] Not included in the training set.

are known to exhibit significant anharmonicities. However, as their frequencies are much lower, corrections for these anharmonicity changes would account for frequency differences of less than 10 cm^{-1}, which in turn is smaller than the root-mean-square (rms) deviation of the calculated frequencies for the training molecules (see below). Thus, in this study we have restricted the anharmonicity corrections to the X−D stretchings.

Anharmonicity constants X_{CH} ($X_{CH} = \omega_{e,CH}x_{e,CH}$) of 58.5 cm^{-1} have been reported for benzene[52] and of 53.9 and 59 cm^{-1} for pyrrole.[53,54] Assuming a mean value for $x_{e,CH}$ of 0.0183, one obtains $(\sigma_{CH})^a = 0.928$ and $(\sigma_{CD})^c = 1.0203$. The anharmonicity constants of the N−H stretching modes exhibit essentially the same value ($X_{NH} \approx 69$ cm^{-1}) in a variety of compounds including secondary amides, lactams, pyrrole, and imidazole.[55] Taking $x_{e,NH} = 0.0190$, the corresponding value for $(\sigma_{NH})^a$ (0.925) is slightly smaller and that for $(\sigma_{ND})^c$ (1.0214) is slightly larger than those for the C−H stretching.

The fitted scaling factors (σ_{XH}) implicitly account for the intrinsic anharmonicities of the C−H and N−H bonds. Thus, the extension of these scaling factors to the deuterated isotopomers requires, independent of the underlying quantum chemical method, just two correction factors, $(\sigma_{CD})^c$ and $(\sigma_{ND})^c$, which convert the scaled diagonal force constants of the C−H and N−H stretchings into the corresponding force constants of the X−D stretchings. The good performance of this approach is illustrated for the N−H/N−D and C−H/C−D stretchings of pyrrole isotopomers (Table 3). The mean deviation is 17 cm^{-1} when the anharmonicity changes upon deuteration are neglected. This is clearly larger than the mean deviation of 11 cm^{-1} averaged over all training set molecules. However, when $(\sigma_{CD})^c = 1.0203$, is adopted, the rms error for the stretching modes is lowered to 10 cm^{-1}. A similar improvement from 31 to 7 cm^{-1} is achieved when the anharmonicity correction is applied to N−D stretchings (Table 4).

Limitations of this approach based on the Morse oscillator model become apparent when experimental values for $x_{e,XD}$ are compared with those derived from the model. For benzene, an $x_{e,CD}$ value of 0.0134 is calculated from eq A6 (Appendix I), while the experimental value is ca. 0.0125.[52] The $x_{e,NH}$ values for *N*-methyl propionamide and pyrrole are 0.0192 and 0.0187, respectively. The predicted values for $x_{e,XD}$ of 0.0140 and 0.0137 have to be compared with the corresponding experimental values of 0.0145 and 0.0111, respectively.[55] Despite these limitations, the Morse oscillator approximation approach appears to account satisfactorily for the anharmonic effects of the X−H/X−D stretchings. In the fit procedure, however, we excluded C−D and N−D stretching frequencies of deuterated isotopomers from

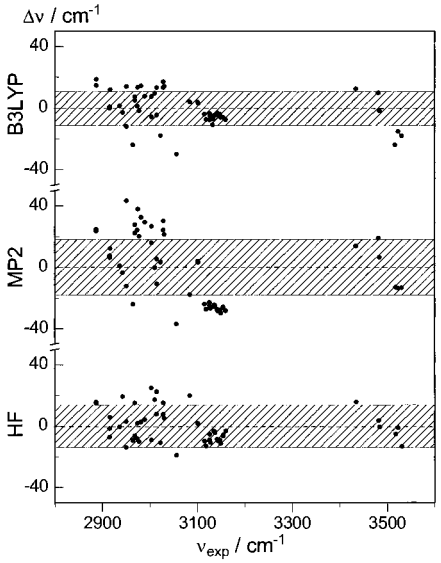

Figure 4. Deviations of the calculated frequencies from the experimental data in the range between 2800 and 3600 cm^{-1}. The calculated frequencies refer to the scaled force fields obtained by HF, MP2, and B3LYP. The shaded areas indicate the respective rms deviations.

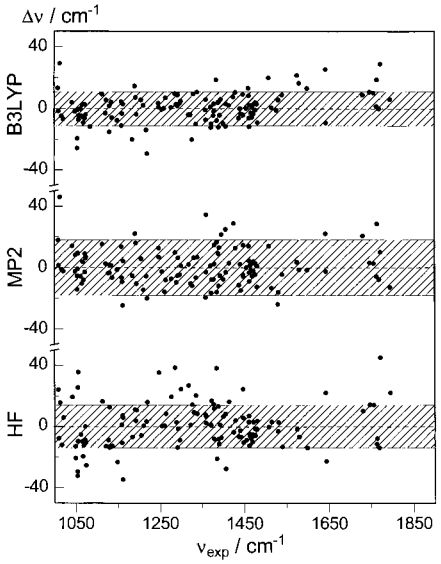

Figure 5. Deviations of the calculated frequencies from the experimental data in the range between 1000 and 1900 cm^{-1}. The calculated frequencies refer to the scaled force fields obtained by HF, MP2, and B3LYP. The shaded areas indicate the respective rms deviations.

the experimental set in order to avoid bias by the use of the fixed relationship eq 5.

Comparison of Calculated and Experimental Frequencies. The mean deviations of the calculated from the experimental frequencies are 11.3 cm^{-1} for B3LYP, 12.9 cm^{-1} for HF, and 17.1 cm^{-1} for MP2. The B3LYP method yields the highest accuracy although it requires the smallest number of scaling factors, i.e., 10 as compared to 14 and 11 for HF and MP2, respectively. Moreover, the accuracy of B3LYP is comparable for the various training molecules. The deviations are somewhat smaller than those obtained by Rauhut and Pulay[29] for a different set of 20 training molecules (rms = 12.8 cm^{-1}) but larger than those obtained by direct scaling of primitive valence force constants (rms = 8.5 cm^{-1}).[51] The quality of the global scaling factors determined in this study is also demonstrated by a comparison with the results obtained by individual fitting. For instance, the rms value for pyrrole is only reduced from 10 to 6 cm^{-1} when a specifically adjusted set of scaling factors is employed for the B3LYP force field.

Comparing the results obtained by the two other methods, it is interesting to note that the accuracy of MP2 is even somewhat lower than that of HF, implying that a sufficiently substantiated set of scaling factors can effectively account for the errors arising from the neglect of electron correlation effects.

Figures 4 and 5 illustrate the accuracies of the various methods. In addition, the deviations for the NH str, NH def and NH oop vibrations, and those of the ND isotopomers are listed in Table 4. Particular attention ought to be paid to these modes for several reasons. First, in oligopyrroles the nitrogen-bound hydrogens can readily be exchanged by deuterium. Second, the NH group is very sensitive to interactions with other molecules, particularly via hydrogen bonding. Third, in all training molecules the NH def internal coordinate contributes significantly to several modes. Hence, several bands are affected upon deuteration.

In the region of the X−H stretching modes (Figure 4), both HF and B3LYP are in a very good agreement with average deviations of ca. 11 cm^{-1}. In contrast, MP2 calculations lead to much larger deviations (23.8 cm^{-1}) which particularly refer to the C−H stretchings rather to the N−H stretching modes. These deviations are systematic inasmuch as the calculated frequencies are generally too low for the unsaturated but too high for the saturated molecules. There is an underestimation of the N−H stretching frequencies for pyrrole, pyrazole, and imidazole at the B3LYP level. This may be due to an overestimation of the N−H bond lengths in these compounds (vide supra). Since the deviations are at most − 23 cm^{-1} (Table 4) and are small in maleimide and uracil, we restrained from introducing a separate NH str scaling factor for B3LYP, in contrast to HF and MP2.

Among the C−H stretchings, there is one remarkable deviation of the B3LYP calculations. It refers to the mode ν_{18} (B_u) of butadiene which is the symmetric C−H stretching of the CH_2 groups. Its frequency is calculated to be 3026 cm^{-1}, but it is observed at 3056 cm^{-1} (Table 5).[67] Moreover, for the corresponding mode ν_2 of A_g symmetry an even higher value of 3027 cm^{-1} is calculated although the deviation from the experimental frequency (3014 cm^{-1}) is still acceptable. This inversion of the calculated modes as compared to the experiment is also obtained by the HF and MP2 calculations which yield frequencies for the ν_2 and ν_{18} modes quite similar to those obtained by the B3LYP method. Close-lying frequencies are also predicted by other force field calculations.[15,67,68,71−73] Evidently, the splitting depends on the size of the basis set and the theoretical method used.[72,73] But even if the correct order is reproduced, the magnitude of the splitting is much smaller than that of the experimental one. Only an empirical force field yields a somewhat larger splitting,[74] suggesting that these deviations reflect a weakness of the quantum chemical calculations. Although this specific defect may be relevant for applying scaled quantum chemical force field calculations in general, it has no impact on our main objective, i.e., the vibrational analysis of tetrapyrroles in chromoproteins where no data of the C−H stretching region are available.

The situation is somewhat different for a second major deviation of the B3LYP calculations which again concerns modes of butadiene and which are indeed located in a spectral region of potential interest for the analysis of the RR spectra of tetrapyrroles. For the mode ν_{10} (A_u), the experimental frequency is at 1013 cm^{-1} whereas the calculated value is higher by 31 cm^{-1} (Table 5). This deviation is accompanied by an inversion of the order of the calculated frequencies for the adjacent modes

TABLE 5: Calculated and Experimental Frequencies (in cm^{-1}) of Butadiene[a]

mode	ν_{exp}[b]	ν_{exp}[c]	B3LYP[d]	$\Delta\nu$	mode composition[e]	B3LYP[f]	HF	MP2
					Ag			
ν_1	3101	3100.3	3105	4	2·32 C_3-H_7 str; 2·17 C_3-H_9 str (CH_2 a-str)	3105	3103	3105
ν_2	3014	3013.0	3027	13	2·31 C_3-H_9 str; 2·14 C_3-H_7 str (CH_2 s-str)	3027	3037	3020
ν_3	3014	3013.0	3010	−4	2·44 C−H str	3010	3022	3003
ν_4	1643	1643.9	1668	25	2·30 C═C str; 10 C−C str	1668	1666	1665
ν_5	1442	1440.8	1438	−4	2·38 CH_2 def	1438	1437	1427
ν_6	1291[g]	1276.5	1291	0	2·20 CH rock; 2·11 C═C str	1291	1278	1286
ν_7	1205	1203.0	1209	4	30 C−C str; 2·13 CH_2 rock; 2·13 CH rock	1209	1202	1211
ν_8	890	887.8	878	−12	45 C−C str; 2·23 CH_2 rock	878	867	876
ν_9	513	511.6	511	−3	2·36 C═C−C def	511	500	512
					A_u			
ν_{10}	1013.2	1014.0	1045	31	2·28 C═C twist, 2·19 CH wag	1018	1030	1059
ν_{11}	907.8	908.1	922	14	2·49 CH_2 wag	922	922	945
ν_{12}	524.5	524.6	529	5	2·22 C═C twist, 2·22 CH wag, 11 C−C tors	516	512	539
ν_{13}	163	162.5	172	9	84 tors	166	150	158
					B_g			
ν_{14}	967	965.4	988	21	2·29 CH wag, 2·21 C═C twist	972	983	1006
ν_{15}	911	908.0	926	15	2·49 CH_2 wag	925	923	946
ν_{16}	753	751.9	768	15	2·28 C═C twist, 2·21 CH wag	748	750	781
					B_u			
ν_{17}	3102	3100.6	3105	3	2·32 C_3-H_7 str, 2·17 C_3-H_9 str (CH_2 a-str)	3105	3104	3105
ν_{18}	3056	3054.8	3026	−30	2·31 C_3-H_9 str, 2·14 C_3-H_7 str (CH_2 s-str)	3026	3037	3019
ν_{19}	3010[g]	2984.1	3020	10	2·44 C−H str	3020	3027	3010
ν_{20}	1599	1596.5	1612	13	2·35 C═C str, 2·13 CH_2 def	1612	1585	1597
ν_{21}	1385	1380.7	1377	−8	2·36 CH_2 def	1377	1365	1369
ν_{22}	1296.2	1294.2	1297	1	2·34 CH rock	1297	1288	1292
ν_{23}	990.6	990.3	986	−5	2·38 CH_2 rock, 2·10 CH rock	986	980	981
ν_{24}	301	301	296	−5	2·47 C═C−C def	296	291	296
rms			13.5			10.8	14.3	20.4

[a] Numbering of the atoms and definition of the internal coordinates are according to Pulay et al.[15] [b] Data which were taken from Bock et al.[67] and used for the global fitting. [c] Taken from ref 68. Further experimental data are reported in refs 69−71. [d] Calculated with the 10-parameter set. [e] Potential energy distributions are given in percentage; only contributions larger than 10% are listed. In the case of two symmetry-equivalent internal coordinates, only one of them is indicated. [f] Calculated with the 10-parameter set but using a specific scaling factor (0.8681) for the torsional coordinates. [g] Corrected for Fermi resonance.

ν_{14} (B_g) and ν_{23} (B_u), observed at 967 and 991 cm^{-1} but calculated at 988 and 986 cm^{-1}, respectively. Both the relatively large deviations of the modes ν_{10} and ν_{14} as well as the inversion of the ν_{14}/ν_{23} mode order have a common origin since the modes ν_{10} and ν_{14} include the same internal coordinates, i.e., the C═C twisting and the C−H oop wagging, albeit with different relative contributions. In terms of potential energy distribution, the C═C twisting character of the modes ν_{10} and ν_{14} is 56% and 42%, respectively, and the positive deviations of the calculated frequencies is 31 and 21 cm^{-1}, respectively. Thus, it is reasonable to assume that these deviations result from the scaling of the torsional force constants, i.e., the global scaling factor σ(conj bond tors) is evidently too large for butadiene. Taking into account that the set of training molecules includes five heterocycles with conjugated bond systems but only one noncyclic conjugated compound, i.e., butadiene, it is evident that this scaling factor optimized in such a way predominantly compensates the errors of the ring torsional force constants. It is concluded therefore that the torsional force constants of butadiene require a specific scaling factor which is smaller than that for the conjugated cyclic compounds. In fact, by using a specific scaling factor of 0.8681 for this force constant of butadiene, the deviations from the experimental frequencies of the modes ν_{10} and ν_{14} are drastically reduced to +5 and +6 cm^{-1}, respectively, and in addition, the experimentally observed order of the modes ν_{23} and ν_{14} is reproduced. Although this specific scaling factor was obtained from a fit based on only seven frequencies and by keeping all other scaling factors constant, the relatively low standard deviation of ±0.0065 compares well with those of the globally optimized scaling factors. Its value is much lower than that for the single bond and conjugated bond torsion (Table 2). When all scaling factors are re-optimized as well, nearly the same value for the butadiene torsional scaling factor (0.8622) is obtained, and the other scaling factors vary by less than 0.2% accompanied by only a marginal improvement of the rms value.

To determine whether the use of a specific scaling factor for noncyclic double bonds is justified, we have calculated the vibrational spectrum of ethene on the basis of both the 10-parameter and the extended 11-parameter scaling factor set. Ethene exhibits only one twisting mode which, due to its symmetry (A_u), is separated from all other modes. It is observed at 1023 cm^{-1} (taken from ref 15), whereas the calculated frequencies are at 1042 and 997 cm^{-1} when scaled with the 10- and 11-parameter sets, respectively. In this case the specific scaling factor for the torsional force constant of the double bond in a noncyclic molecule yields an even larger deviation from the experimental value (−26 cm^{-1}) than that obtained with the standard 10-parameter set (+19 cm^{-1}). Thus, it appears that the introduction of the additional scaling factor for a double bond torsion may only be required for linear polyenes. Whether in this regard the exocyclic double bonds in the target molecules, i.e., the methine bridges and the vinyl substituents, can be regarded as isolated (ethene-like) or as conjugated double bonds (butadiene-like) remains to be checked by the vibrational analyses of dipyrrolic test molecules.

Similar systematic deviations for the butadiene CH oop modes are also noted for the MP2 calculation (Table 5). Also in this case, a specific scaling factor for the butadiene torsional coordinates leads to a substantial improvement. The optimized value of this scaling factor, obtained by keeping all other scaling factors unchanged, is 0.8440 ± 0.0083 which happens to be

TABLE 6: Selected Structural and Spectral Data for Maleimide Monomer and Dimer

Bond Lengths (Å)

	experimental[a]			calculated (B3LYP)		
	monomer	dimer	ΔR_{exp}	monomer	dimer	ΔR_{calc}
C(2)−N	1.409	1.375	−0.034 (−0.043)[b]	1.398	1.381	−0.017
C(2)−O	1.206	1.226	0.020 (0.011)[b]	1.212	1.224	0.012
N−H				1.011	1.026	0.015

Frequencies of NH Modes (cm^{-1})

	experimental[c]			calculated (B3LYP)[d]		
	monomer	dimer	$\Delta \nu_{exp}$	monomer	dimer	$\Delta \nu_{calc}$
NH str	3486	3255	−231	3492	3264	−228
NH def	1346	1360	+14	1328	1394 (1350)	+66 (+22)
NH oop	505	740	+235	521	807 (734)	+286 (+213)

[a] The experimental data were taken from refs 42 and 34 for the gas-phase structure (monomer) and crystal structure (mean values of dimers), respectively. [b] Unpublished X-ray data from our laboratory. [c] The experimental data refer to Ar matrix IR spectra.[61] [d] Values in parentheses were obtained by employing specific scaling factors of 0.89 and 0.83 for the deformation and out-of-plane force constants, respectively.

nearly the same as the scaling factor for the single bond torsion (0.8488). Using this latter scaling factor for the butadiene torsional coordinates, the subsequent reoptimization of all scaling factors reduces the total rms error from 17.1 to 16.5 cm^{-1}. Since this improvement is just due to the better agreement for the butadiene CH oop modes, i.e., due to a molecule-specific scaling, we retained the original set of global scaling factors for MP2 as in the case of B3LYP (Table 2).

For the B3LYP-calculated frequencies, there are three further relatively large deviations which, however, appear to arise from the lack of reliable experimental data. The IR-inactive CH oop mode (A_2) of ND-pyrrole was assigned to a Raman band of the liquid sample observed at 712 cm^{-1}.[56] For a comparison with the calculated frequency at 668 cm^{-1}, a correction for the "gas-liquid" shift was employed for which a value of −9 cm^{-1} has been estimated by Orza et al.[75] Then the corrected frequency corresponds to a deviation of −35 cm^{-1}. However, this correction appears to be too small in view of the substantially larger "gas-liquid" shift (−21 cm^{-1}) of pyrrole which could be determined experimentally.[57] Adopting this −21-cm^{-1} correction also for the CH oop mode of ND-pyrrole reduces the deviation to −23 cm^{-1}. This value is still relatively large. However, we note that similar deviations are associated with some modes of the same symmetry although they are not systematic for the CH oop modes. For the observed oop modes of 12 asymmetrically deuterated pyrroles ($A_2 \rightarrow A''$), the B3LYP force field yields a mean deviation of no more than 11 cm^{-1}, which is essentially the same as the rms value for the complete set of training molecules.

For the ring torsional modes of maleimide and *N*-deuterated maleimide the B3LYP calculations yield deviations of −30 and −42 cm^{-1}, respectively. The corresponding experimental IR data (163 and 175 cm^{-1}, respectively) were taken from measurements of benzene solutions and polyethylene pellets, i.e., nonpolar solvents.[60] It is likely that under these conditions maleimide forms dimers similar to the solid state.[34] B3LYP calculations indicate that dimer formation has a pronounced effect on this torsional mode which shifts up from 133 to 151 cm^{-1} in both the nondeuterated and the deuterated species. If these values are compared with the experimental data, the deviations are substantially reduced to −12 and −24 cm^{-1}, respectively.

Effect of Hydrogen Bonding. Molecules which include proton donating and accepting functions such as imino and carbonyl groups can be subject to strong hydrogen bonding interactions which affect the molecular structures and frequencies. This is true for several compounds of the sets of training, test, and target molecules studied in this work. Therefore, these effects require special attention, particularly, since it was shown by Del Bene et al.[66] that B3LYP failed to predict reliable binding energies, intermolecular distances, and frequency shifts of the X−H stretchings induced by hydrogen bonding for a variety of small hydrogen-bonded complexes.

The tetrapyrrole target molecules may undergo inter- and intramolecular hydrogen bonding interactions. In the crystalline state, BVE forms centrosymmetric dimers via intermolecular hydrogen bonding between the NH group of a peripheral ring of one molecule and the C═O group of a second molecule.[17] For a model compound of PCB, Kratky et al.[76] demonstrated that such interactions occur at ring D. To assess the structural and spectral consequences of these hydrogen bonding interactions we have chosen maleimide as a model compound for ring D of PCB (corresponding to either rings A and D of BVE) and extended the B3LYP calculations to the dimeric entity of maleimide.

The geometry optimization yields a dimeric structure of C_i symmetry. This calculated structure as well as that of the monomer can be compared with experimental data, i.e., the gas-phase structure (monomer) obtained by electron diffraction[42] and the dimeric structure available from X-ray crystallography.[34] The main differences Δ_{exp} between the experimentally determined structures concern a shortening of the C(2)−N bond and an elongation of the C(2)═O bond in the crystal (Table 6). In fact, the calculations largely reproduce these changes although ΔR_{exp}(C(2)−N) is larger by 0.02 Å than the difference for this coordinate between the calculated dimer and monomer structures (ΔR_{calc}). This quantitative discrepancy is due to a slight underestimation of the calculated bond length in the monomer and an overestimation of this coordinate in the dimer. In addition, the calculations reveal the expected increase of the N−H bond length in the dimer.

As expected, the most pronounced effects of hydrogen bonding on the vibrational spectra are noted for the N−H stretching modes (downshift) and the N−H def and oop modes (upshift) (Table 6). The calculated values for the monomers agree very well with the corresponding experimental data, and

TABLE 7: Calculated and Experimental Infrared and Raman Intensities of Butadiene[a]

	experimental		B3LYP/6-31G*		B3LYP/6-31++G**		HF/6-31G*		MP2/6-31G*	
mode	I_{IR}[b]	I_{Ra}[c]	I_{IR}	I_{Ra}	I_{IR}	I_{Ra}	I_{IR}	I_{Ra}	I_{IR}	I_{Ra}
					A_g					
ν_1		56		32.3		18.8		21.9		73.0
ν_2		76		40.9		29.2		29.2		114.5
ν_3				11.8		6.1		3.9		25.2
ν_4		100		100.0		100.0		100.0		100.0
ν_5		17		25.6		14.5		18.0		52.3
ν_6		12[d]		37.0		27.9		39.4		48.3
ν_7		20		30.3		22.1		24.3		61.0
ν_8				0.3		0.8		0.5		0.3
ν_9		19		21.2		13.0		14.7		29.3
					A_u					
ν_{10}	32.4		26.2		40.6		29.9		43.7	
ν_{11}	63.01		78.5		94.7		102.4		75.5	
ν_{12}	16.18		7.7		13.4		12.2		9.5	
ν_{13}			0.2		0.7		0.1		0.2	
					B_g					
ν_{14}				3.1		3.2		5.6		2.6
ν_{15}				3.6		11.6		7.3		2.3
ν_{16}				23.0		3.6		23.4		65.9
					B_u					
ν_{17}	28.5		33.1		27.9		44.6		23.1	
ν_{18}	12.8		8.5		9.7		17.4		4.4	
ν_{19}	10.9[d]		31.9		25.9		28.7		22.2	
ν_{20}	17.33		12.4		23.6		17.2		6.6	
ν_{21}	2.96		2.6		3.1		1.3		3.8	
ν_{22}	1.94		2.3		2.5		2.9		2.2	
ν_{23}	1.7		2.3		2.6		2.3		2.6	
ν_{24}			2.6		2.6		3.4		2.0	
$\Delta I/I_{exp}$[e]			27	35	27	29	37	30	37	105
rms			6.8		11.2		14.4		7.8	

[a] IR intensities are given in km/mol; Raman intensities are given as relative intensities with respect to the strongest band (ν_4). [b] Taken from ref 68. [c] Taken from ref 80; the intensity values were normalized with respect to the strongest band (ν_4). [d] Intensities perturbed by Fermi resonance. [e] Relative deviation given in percentage. The modes ν_{19} and ν_6 were not included. See text for further explanations.

the shifts induced by dimerization are reproduced qualitatively as well. However, the absolute values for the dimers display substantial deviations with regard to the experimentally determined frequencies. These deviations can readily be removed by modifying the scaling factors for the NH def and NH oop internal coordinates. While in this particular case of the maleimide dimer the NH str coordinate needs no adjustment, substantial modifications are needed for the NH def (from 0.9693 to 0.89) and NH oop (from 1.0120 to 0.83). Similar results were obtained for other representatives of the sets of training and test molecules, implying that hydrogen bonding interactions may require specific scaling factors for the NH modes.

IV. Intensities. For the test and target molecules, the number of normal modes in the spectral region between 200 and 1800 cm^{-1} is between 100 and 150 corresponding to an average "mode density" of up to 1 mode per 10 cm^{-1}. Even for an accuracy of the frequency calculation between 10 and 15 cm^{-1}, the spectra analysis of such large molecules would not provide unambiguous results in many cases. Hence, we have calculated IR, Raman, and RR intensities in order to gain further criteria for the band assignments.

The matrix elements of the dipole moment derivatives which determine the IR intensities are evaluated efficiently in the GAUSSIAN94 program by means of analytical methods. In contrast, the algorithm implemented for the calculation of the polarizability derivatives, which are required for evaluating Raman intensities is prohibitively time-consuming for large molecules. We have therefore employed an alternative approach which is described in detail in Appendix II. In brief, for off-resonance excitation (ν_0), the Raman intensity $I_{Ra,s}$ of a normal mode s with the frequency ν_s is given by eq 6,[77]

$$I_{Ra,s} \propto (45(\alpha')^2 + 7(\gamma')^2)\frac{(\nu_0 - \nu_s)^4}{\nu_s\left(1 - \exp\left(-\frac{h\nu_s}{kT}\right)\right)} \qquad (6)$$

where α' and γ' are the derivatives of the mean polarizability α and its anisotropy γ with respect to the normal mode *s*. Equation 6 refers to a setup with the incident light in the *x*-direction, being linearly polarized in the *z*-direction, and the scattered light observed in the *y*-direction. Using the finite electric field method,[78] the derivatives α' and γ' were evaluated by 2-fold numerical differentiation of the forces acting on the atoms with respect to an applied electric field. To obtain numerically accurate Raman intensities, it was essential to use an algorithm which effectively minimizes the errors associated with the numerical differentiation as well as those arising from other sources (Appendix II).

Comparison of Calculated and Experimental IR Intensities. In general, there is good agreement between the calculated and experimental IR intensities. As an example, we wish to discuss the spectra of butadiene for which experimental data are available (Table 7).[68] For this molecule, only the A_u and B_u modes are IR active. The inspection of the data reveals that there is one major deviation. It concerns the mode ν_{19} which has been found to be perturbed by Fermi resonance.[67] As a quantitative measure for comparing calculated and experimental intensities one may use either the relative deviation $\Delta I/I_{exp}$ that weights more strongly deviations for bands of weak intensities, or the rms error giving greater weight to deviations of strong

bands. Neglecting the mode ν_{19}, it is evident that according to both criteria the B3LYP method provides the best agreement whereas the HF and MP2 results yield similar relative deviations. The rms error for HF is larger compared to MP2 which is essentially due to the relatively strong deviation for the mode ν_{11}.

In view of the good performance of B3LYP for IR intensity calculations, one would also expect a good agreement for the dipole moments, which is in fact confirmed for those molecules for which reliable experimental data are available, for instance, pyrrole, $\mu_{calc} = 1.91$ D, $\mu_{exp} = 1.74$ D[35] (1.84[81]); pyrazole, $\mu_{calc} = 2.29$ D, $\mu_{exp} = 2.21$ D;[37] imidazole, $\mu_{calc} = 3.72$ D, $\mu_{exp} = 3.67$ D;[36] propane, $\mu_{calc} = 0.06$ D, $\mu_{exp} = 0.08$ D.[40] In this respect, the present results are in line with a recent study by De Proft et al.[28] who also found that B3LYP leads to semiquantitative predictions for the IR intensities, and to a good agreement for the dipole moments. The latter, however, could be definitely improved by employing a triple-ζ polarization basis set.

According to Miller et al.,[82] a better performance for IR intensity calculations can be obtained by using a 6-31++G** basis set which includes polarization functions for the hydrogens and diffuse functions and yet is still a relatively compact basis set. In the case of butadiene, such an improvement was not found for the B3LYP calculation, as the relative deviation is basically the same and the rms error is even increased, mainly because for the strongest IR band (ν_{11}) the calculated intensity is much too large so that the slightly better agreement for the remaining modes is overridden. For ethane, however, the 6-31++G** basis set leads to a substantial improvement as compared to the 6-31G* basis set.

Comparison of Calculated and Experimental RAMAN Intensities. It has been shown that accurate Raman intensity calculations require large basis sets including diffuse and polarization functions.[83] Hence, it is quite remarkable that B3LYP and HF reproduce the experimental data in a qualitative way (Table 7). For the Raman-active A_g and B_g modes of butadiene, we note two major deviations for all methods. The experimentally observed Raman intensity of mode ν_6 is probably weakened by a Fermi resonance. As a consequence, the calculated intensities of this mode are too high. A similar overestimation has been already mentioned for the equally perturbed IR-active mode ν_{19}. In addition, a considerable Raman intensity is calculated with the 6-31G* basis set for the mode ν_{16} which, however, has no counterpart in the experimental spectrum. On the B3LYP level, this deviation is substantially reduced by using the 6-31++G** basis set, although the agreement for the remaining Raman-active modes is not significantly improved.

The hydrogen-bonded maleimide dimer represents a second instructive example for the comparison between the experimental and calculated Raman spectra (Figure 6). The vibrational assignments which are based on the IR and Raman spectra will be discussed in detail elsewhere.[30a] In the region below 1900 cm^{-1}, the B3LYP calculations provide a good agreement with the experimental data even for the 6-31G* basis set. The intensity pattern is nicely reproduced although for some modes for which the experiment reveals relatively weak intensities, the calculated intensities are somewhat too high. These deviations are reduced with the 6-31++G** basis set which gives a better agreement for the weaker Raman bands. Serious deviations, however, are noted in the region of the C−H and N−H stretching modes, the calculated intensities of which are far too high. This is particularly true for the N−H stretching (ν_1). The

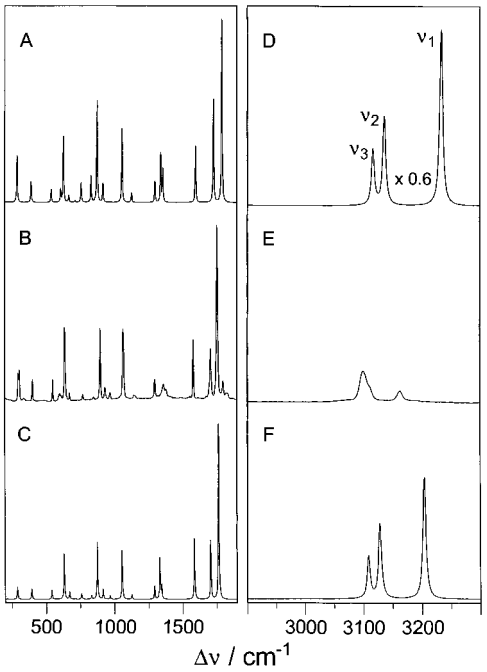

Figure 6. Experimental and calculated Raman spectra of maleimide. A, D, Raman spectrum of the dimer calculated with B3LYP and 6-31G* basis set; C, F, Raman spectrum of the dimer calculated with B3LYP and 6-31++G** basis set; B, E, experimental Raman spectrum of the solid obtained with 1064-nm excitation at ambient temperature; further experimental details will be given elsewhere.[30a] The intensity scale of D is reduced by a factor of 0.6 relative to A.

6-31G* basis set yields an intensity which is even three times higher than that of the mode ν_3. In contrast, the intensity ratio ν_1/ν_3 in the experimental spectrum is less than 0.1. Again, the larger basis set leads to an improvement as the relative intensities of the N−H and C−H stretching modes are substantially reduced with respect to the most intense band in the experimental spectrum at ca. 1760 cm^{-1}. This result is not unexpected since the inclusion of polarization functions for the hydrogen atoms and of diffuse functions should provide the greatest relative improvement for the description of the hydrogen atoms. Hence, this should have a particularly strong impact on those modes which are dominated by vibrations involving hydrogen atoms.

In general, however, the examples discussed in this work as well as the results we have obtained for other training and test molecules indicate that even with the 6-31G* basis set B3LYP calculations can yield satisfactory semiquantitative Raman intensities. In combination with the calculated IR intensities, they can serve as valuable additional criteria for the vibrational assignments of medium-size molecules.

For molecules of the size of the training and test molecules, nonresonant conditions for measuring the Raman spectra can readily be established. The situation is different for the target molecules since due to their extended π-electron systems they exhibit strong electronic transitions in the visible range of the spectrum. Hence, even near-infrared excitation (1064 nm) always provides a substantial preresonance enhancement so that eq 6 is not adequate for calculating the Raman intensities. Thus, we have also calculated RR intensities using the "bond order" approximation according to Peticolas and co-workers.[84] This approach, which has already been employed in our previous semiempirical study,[16] gives at least reasonable estimates for

those modes which are dominated by the stretching vibrations of the chromophoric skeleton.

Conclusions

We have developed a three-step strategy for calculating vibrational spectra of linear tetrapyrroles which serve as prosthetic groups in various chromoproteins. In contrast to cyclic tetrapyrroles, i.e., porphyrins, no symmetry selection rules facilitate the spectra analysis of these molecules. Thus, particularly high demands are imposed on the accuracy and reliability of the present approach.

These requirements were best fulfilled by the B3LYP method. Deviations of the calculated structures approach the accuracy of the experimental methods. The mean deviation of 11.3 cm^{-1} for the frequency calculations corresponds to the range of frequency variations induced by hydrophobic or electrostatic interactions as they are noted, e.g., in the IR spectra measured in KBr pellets, CCl_4 solutions, and Ar matrixes. Such "environmental" effects were not taken into account in the calculations. In addition, within the set of training molecules the rms error does not depend on the size of the molecules, i.e., neither on the number of heavy atoms nor the total number of atoms. Thus, one may expect a comparable accuracy for the frequency determination also for larger molecules including linear tetrapyrroles.

For such large molecules the calculated IR and Raman intensities are necessary additional criteria for the vibrational assignments. The lack of a sufficiently large body of standardized experimental data does not allow a quantitative assessment of accuracy of the intensity calculations. However, as far as a comparison with measured spectra was possible, a semiquantitative prediction, i.e., classification in terms of very strong, strong, medium, weak, and very weak bands, of both the IR and the Raman intensities was achieved. A specific difficulty of the vibrational analysis of linear tetrapyrroles is associated with their capability to form hydrogen bonds. Such intermolecular interactions are likely to play an important role also for the protein-bound chromophores. Special emphasis was therefore laid on the analysis of the impact of hydrogen bonding interactions on the accuracy of the calculated structural and spectral data. It was found that, in general, the calculations can qualitatively predict the consequences of hydrogen bonding interactions on the molecular structures and vibrational spectra. However, to maintain the required accuracy of the frequency calculations, specific scaling factors have to be adopted for the force constants of the N−H stretching, bending, and oop wagging. It remains to be shown whether these scaling factors are transferable to molecular systems of different hydrogen bond geometries and strengths. Regardless of this uncertainty, however, it can be concluded that the present approach holds promise to provide calculated spectra of linear tetrapyrroles which allow for a reliable vibrational assignment of most of the observed bands and, hence, may contribute substantially to the interpretation of the RR spectra of the protein-bound chromophores.

Acknowledgment. P. H. gratefully acknowledges a Heisenberg Fellowship by the Deutsche Forschungsgemeinschaft. We thank Dr. C. Kneip for measuring the Raman spectrum of maleimide.

Appendix I: Anharmonicity Corrections

The derivation of the anharmonicity correction is based on (i) the Morse model for an anharmonic oscillator[85] and (ii) on the assumption that the scaling factor can be factorized into an anharmonic (σ^a) and a quantum chemical contribution (σ^q) (see eq 2). We will consider specifically an X−H and X−D oscillator, but the results can be easily generalized to other isotopomers.

The force constant for a harmonic oscillator is given by eq A1,

$$(F_{XH})^h = \mu_{XH}\,(2\pi\omega_{e,XH})^2 \tag{A1}$$

where μ_{XH} is the reduced mass and $\omega_{e,XH}$ the harmonic frequency which is related to the anharmonic frequency ν_{XH} of the first vibrational level of a Morse oscillator according to eq A2.

$$\nu_{XH} = \omega_{e,XH}(1 - 2x_{e,XH}) \tag{A2}$$

The anharmonicity constant $x_{e,XH}$ depends on the potential parameter and on $\omega_{e,XH}$.[86] For the effective force constant $(F_{XH})^{eff}$ which refers to ν_{XH} one obtains from eqs A1 and A2

$$(F_{XH})^{eff} = \mu_{XH}(1 - 2x_{e,XH})^2(2\pi\omega_{e,XH})^2 \tag{A3}$$

The scaling factors are optimized in such a way that the calculated (harmonic) frequencies match the observed (anharmonic) frequencies, which implies that the scaled force constant $(F_{XH})^{\sigma}$ (see eq 5) equals the true (anharmonic) force constant $(F_{XH})^{eff}$, i.e.,

$$(F_{XH})^{eff} = (F_{XH})^{\sigma} = (\sigma_{XH})^q(\sigma_{XH})^a F_{XH} = (\sigma_{XH})^a(F_{XH})^h \tag{A4}$$

Insertion of eqs A1 and A3 into eq A4 yields eq A5

$$(\sigma_{XH})^a = (1 - 2x_{e,XH})^2 \tag{A5}$$

In an analogous way, one obtains $(\sigma_{XD})^a$ for the force constant of the X−D vibration, taking into account that within the Morse potential approximation $x_{e,XD}$ is related to $x_{e,XH}$ according to

$$x_{e,XD} = x_{e,XH}\sqrt{\frac{\mu_{XH}}{\mu_{XD}}} \tag{A6}$$

so that eq A7 is readily obtained,

$$(\sigma_{XD})^a = \left(1 - 2x_{e,XH}\sqrt{\frac{\mu_{XH}}{\mu_{XD}}}\right)^2 \tag{A7}$$

Finally, a correction factor $(\sigma_{XD})^c$ is introduced which is given by the ratio of the anharmonic corrections of the XD and XH oscillators,

$$(\sigma_{XD})^c = \frac{(\sigma_{XD})^a}{(\sigma_{XH})^a} \tag{A8}$$

Combining eqs A5, A7, and A8 yields the explicit expression for $(\sigma_{XD})^c$ in eq 3.

Appendix II: Raman Intensities

According to eq 6, the Raman intensity $I_{Ra,s}$ of the sth fundamental is related to the derivatives of the polarizability $\alpha'$and its anisotropy γ' with respect to the sth normal mode, where α and γ are given by eqs A9 and A10, respectively:

$$\alpha = \frac{1}{3}(\alpha_{xx} + \alpha_{yy} + \alpha_{zz}) \quad \text{(A9)}$$

$$(\gamma)^2 = \frac{1}{2}[(\alpha_{xx} - \alpha_{yy})^2 + (\alpha_{yy} - \alpha_{zz})^2 + (\alpha_{zz} - \alpha_{xx})^2 + 6((\alpha_{xy})^2 + (\alpha_{yz})^2 + (\alpha_{xz})^2)] \quad \text{(A10)}$$

These derivatives are obtained from the derivatives of the polarizability components α_{ij} ($i,j = x, y, z$) with respect to the Cartesian axes X, i.e., $\partial\alpha_{ij}/\partial X = (\alpha_{ij})'$, after transformation to normal coordinates. The Cartesian derivatives $(\alpha_{ij})'$ are calcu lated according to eq A11,[78]

$$(\alpha_{ij})' = \frac{\partial^2 F_X}{\partial E_i \partial E_j} \quad \text{(A11)}$$

where E_i and E_j are the components of the incident electrical field in i and j direction and F_X the (analytically evaluated) forces acting on the atoms of the molecule induced by the electrical field.

The numerical calculation of $(\alpha_{ij})'$ is associated with errors from different sources: (i) a truncation error due to the neglect of higher order terms in the Taylor expansion of the differentiation formula, (ii) a cancellation error due to the loss of significant digits upon calculating differences, (iii) an integration error due to the grid approximation in the numerical integration of matrix elements in the B3LYP method, (iv) an error due to the incomplete geometry optimization resulting in nonnegligible residual forces at the atoms. The reduction of the effect of the errors ii, iii, and iv requires relatively large values of forces which, however, may cause an increase of the truncation error (i) for a low-order differentiation formula.

In the present approach we have employed a relatively large step size for E_i and a fourth-order differentiation formula which besides its accuracy has the additional advantage to allow an assessment of the errors due the numerical differentiation. This procedure consists of three steps. First, the second-order derivatives of the forces F_X, or of a general function f, i.e., $\partial^2 f/\partial E_i \partial E_j = (f_{ij})''$, are calculated for chosen values of $E = E_i = E_j$ using the well-known second order differentiation formulas,[87] i.e.,

$$(f_{ii}(E))'' = \frac{1}{E^2}[f(+E) - 2f(0) + f(-E)] + O(E^2) \quad \text{(A12)}$$

and

$$(f_{ij}(E))'' = \frac{1}{2E^2}\Delta(E) + O(E^2) \quad \text{(A13)}$$

where $\Delta(E)$ is defined by

$$\Delta(E) = f(E_i,E_j) + f(-E_i,-E_j) + 2f(0,0) - f(E_i,0) - f(-E_i,0) - f(0,E_j) - f(0,-E_j) \quad \text{(A14)}$$

An explicit expression for the error term $O(E^2)$ in eqs A12 and A13 is given elsewhere.[88]

In the second step, the value for E is doubled to calculate the quantities $(f_{ii}(2E))''$ and $(f_{ij}(2E))''$ according to eqs A12, A13, and A14. Finally, more accurate values $\langle f_{ii}\rangle''$ and $\langle f_{ij}\rangle''$ are obtained from

$$\langle f_{ii}\rangle'' = \frac{1}{3}(4(f_{ii}(E))'' - (f_{ii}(2E))'') = (f_{ii})'' - \frac{8}{6!}(f_{iiiiii})''''''E^4 + \ldots \quad \text{(A15)}$$

and

$$\langle f_{ij}\rangle'' = \frac{1}{3}(4(f_{ij}(E))'' - (f_{ij}(2E))'') = (f_{ij})'' - \frac{4}{6!}R(f'''''')E^4 + \ldots \quad \text{(A16)}$$

where the remainder term R(f'''''') contains sixth-order mixed derivatives.

While eq A15 corresponds to a formula published previously,[89] eq A16 is derived from eq A13 by inserting the Taylor expansions for the function values $f(E_i,E_j)$ at the different grid points into the expansions $\Delta(E)$ and $\Delta(2E)$ (eq A14). These expansions which were carried out up to the sixth order were combined with appropriate weighting so that the fourth-order terms cancel.

Instead of Eq (A14), one may use the symmetric function $\Delta'(E) = f(E_i,E_j) + f(-E_i,-E_j) - f(E_i,-E_j) - f(-E_i,E_j)$ involving two additional off-axis points for deriving an expression analogous to eq A16. Such a formula has been reported in an equivalent form by Kurtz et al.[90] The slightly higher accuracy associated with this symmetric function, however, does not justify the increase of the computational effort by ca. $^1/_3$.

The values for E were chosen such that the maximum value of the electric-field induced change of the forces at the atoms was at least 2 orders of magnitude larger than that of the residual forces for the unperturbed structure. Taking into account that even within the TIGHT option for the geometry optimization, maximum residual forces of ca. 0.001 au may exist, we generally used an E value of 0.004 au, whereas greater values may cause SCF convergence problems in particular in the case of large molecules such as tetrapyrroles.

Comparing the values determined for $(f_{ii}(E))''$, $(f_{ij}(E))''$, $\langle f_{ii}\rangle''$, and $\langle f_{ij}\rangle''$, it is possible to estimate the error of the numerical differentiation. It was found that the accuracy of the calculated polarizability derivatives was better than 1% for numerically large matrix elements but lower for very small matrix elements.

References and Notes

(1) (a) Scheer, H. *Angew. Chem., Int. Ed. Engl.* **1981**, *20*, 241. (b) Schaffner, K.; Braslavsky, S. E.; Holzwarth, A. R. In *Frontiers in Supramolecular Organic Chemistry and Photochemistry*; Schneider, H. J., Dürr, H., Eds.; VCH: Weinheim, 1991; p 421.

(2) (a) Holzwarth, A. R. *Q. Rev. Biophys.* **1989**, *22*, 239. (b) MacColl, R.; Guard-Friar, D. *Phycobiliproteins*; CRC Press: Boca Raton, FL, 1987.

(3) (a) Schaffner, K.; Braslavsky, S. E.; Holzwarth, A. R. *Adv. Photochem.* **1990**, *15*, 229. (b) Sineshchekov, V. A. *Biochim. Biophys. Acta* **1995**, *1228*, 125.

(4) (a) Fodor, S. P. A.; Lagarias, J. C.; Mathies, R. A. *Photochem. Photobiol.* **1988**, *48*, 129. (b) Farrens, D. L.; Holt, R. E.; Rospendowski, B. N.; Song, P.-S.; Cotton, T. M. *J. Am. Chem. Soc.* **1989**, *111*, 9162. (c) Fodor, S. P. A.; Lagarias, J. C.; Mathies, R. A. *Biochemistry* **1990**, *29*, 11141. (d) Tokutomi, S.; Mizutani, Y.; Anni, H.; Kitagawa, T. *FEBS Lett.* **1990**, *269*, 341. (e) Mizutani, Y.; Tokutomi, S.; Aoyagi, K.; Horitsu, K.; Kitagawa, T. *Biochemistry* **1991**, *30*, 10693. (f) Hildebrandt, P.; Hoffmann, A.; Lindemann, P.; Heibel, G.; Braslavsky, S. E.; Schaffner, K.; Schrader, B. *Biochemistry* **1992**, *31*, 7957. (g) Mizutani, Y.; Tokutomi, S.; Kitagawa, T. *Biochemistry* **1994**, *33*, 153.

(5) (a) Matysik, J.; Hildebrandt, P.; Schlamann, W.; Braslavsky, S. E.; Schaffner, K. *Biochemistry* **1995**, *34*, 10497. (b) Andel, F., III; Lagarias, J. C.; Mathies, R. A. *Biochemistry* **1996**, *35*, 15997.

(6) (a) Li, X.-Y.; Czernuszewicz, R. S.; Kincaid, J. R.; Su, Y. O.; Spiro, T. G. *J. Phys. Chem.* **1990**, *94*, 31. (b) Li, X.-Y.; Czernuszewicz, R. S.; Kincaid, J. R.; Stein, P.; Spiro, T. G. *J. Phys. Chem.* **1990**, *94*, 47. (c) Li, X.-Y.; Czernuszewicz, R. S.; Kincaid, J. R.; Spiro, T. G. *J. Am. Chem. Soc.* **1991**, *111*, 7012.

(7) Li, X.-Y.; Zgierski, M. Z. *J. Phys. Chem.* **1991**, *95*, 4268.

(8) Yang, B.; Taylor, R. C.; Morris, M. D.; Wang, X.-Z.; Wu, J.-G.; Yu, B.-Z.; Xu, G.-X.; Soloway, R. D. *Spectrochim. Acta* **1993**, *49A*, 1735.
(9) Grossjean, M. F.; Tavan, P.; Schulten, K. *J. Phys. Chem.* **1990**, *94*, 8059.
(10) (a) Kozlowski, P. M.; Zgierski, M. Z.; Pulay, P. *Chem. Phys. Lett.* **1995**, *247*, 379. (b) Kozlowski, P. M.; Jarzecki, A. A.; Pulay, P. *J. Phys. Chem.* **1996**, *100*, 7007. (c) Kozlowski, P. M.; Jarzecki, A. A.; Pulay, P.; Li, X.-Y.; Zgierski, M. Z. *J. Phys. Chem.* **1996**, *100*, 13985.
(11) Jarzecki, A. A.; Kozlowski, P. M.; Pulay, P.; Ye, B.-H.; Li, X.-Y. *Spectrochim. Acta* **1997**, *A53*, 1195.
(12) Braun, D.; Ceulemans, A. *J. Phys. Chem.* **1995**, *99*, 11101.
(13) Fogarasi, G.; Pulay, P. In *Vibrational Spectra and Structure*; Durig, J. R., Ed.; Elsevier: Amsterdam, 1985; Vol. 14, p 125.
(14) (a) Pople, J. A.; Scott, A. P.; Wong, M. W.; Radom, L. *Isr. J. Chem.* **1993**, *33*, 345. (b) Scott, A. P.; Radom, L. *J. Phys. Chem.* **1996**, *100*, 16502.
(15) Pulay, P.; Fogarasi, G.; Pongor, G.; Boggs, J. E.; Vargha, A. *J. Am. Chem. Soc.* **1983**, *105*, 7037.
(16) Smit, K.; Matysik, J.; Hildebrandt, P.; Mark, F. *J. Phys. Chem.* **1993**, *97*, 11887.
(17) Sheldrick, W. S. *J. Chem. Soc., Perkin Trans.* **1976**, *2*, 1457.
(18) (a) Knipp, B.; Kneip, K.; Matysik, J.; Gärtner, W.; Hildebrandt, P.; Braslavsky, S. E.; Schaffner, K. *Chem. Eur. J.* **1997**, *3*, 363. (b) Matysik, J.; Hildebrandt, P.; Smit, K.; Korkin, A.; Mark, F.; Gärtner, W.; Braslavsky, S. E.; Schaffner, K.; Schrader, B. *J. Mol. Struct.* **1996**, *348*, 225.
(19) Seeger, D. M.; Korzeniewski, C.; Kowalchyk, W. *J. Phys. Chem.* **1991**, *95*, 6871.
(20) Trull, F. R.; Ma, J.-S.; Landen, G. L.; Lightner, D. A. *Isr. J. Chem.* **1983**, *23*, 211.
(21) Sheldrick, W. S. *Isr. J. Chem.* **1983**, *23*, 155.
(22) Becke, A. D. *J. Phys. Chem.* **1993**, *98*, 5648.
(23) Bauschlicher, C. W., Jr. *Chem. Phys. Lett.* **1995**, *246*, 40.
(24) Martin, J. M. L.; El-Yazal, J.; François, J.-P. *Mol. Phys.* **1995**, *86*, 1437.
(25) Wong, M. W. *Chem. Phys. Lett.* **1996**, *256*, 391.
(26) El-Azhary, A. A.; Suter, H. U. *J. Phys. Chem.* **1996**, *100*, 15056.
(27) Choi, C. H.; Kertesz, M. *J. Phys. Chem.* **1996**, *100*, 16530.
(28) De Proft, F.; Martin, J. M. L.; Geerlings, P. *Chem. Phys. Lett.* **1996**, *250*, 393.
(29) Rauhut, G.; Pulay, P. *J. Phys. Chem.* **1995**, *99*, 3093.
(30) (a) Németh, K.; Magdó, I.; Hildebrandt, P.; Mark, F. Manuscript in preparation. (b) Németh, K.; Heinemann, O.; Hildebrandt, P.; Mark, F. Manuscript in preparation.
(31) Frisch, M. J.; Trucks, G. W.; Schlegel, H. B.; Gill, P. M. W.; Johnson, B. G.; Robb, M. A.; Cheeseman, J. R.; Keith, T.; Petersson, G. A.; Montgomery, J. A.; Raghavachari, K.; Al-Laham, M. A.; Zakrzewski, V. G.; Ortiz, J. V.; Foresman, J. B.; Peng, C. Y.; Ayala, P. Y.; Chen, W.; Wong, M. W.; Andres, J. L.; Replogle, E. S.; Gomperts, R.; Martin, R. L.; Fox, D. J.; Binkley, J. S.; Defrees, D. J.; Baker, J.; Stewart, J. J. P.; Head-Gordon, M.; Gonzalez, C.; Pople, J. A. *GAUSSIAN 94*, Revision B.3; Gaussian, Inc.: Pittsburgh, PA, 1995.
(32) Goddard, R.; Heinemann, O.; Krüger, C.; Magdó, I.; Mark, F.; Schaffner, K. *Acta Crystallogr.* **1998**, *C54*, 501.
(33) (a) Schmidt, P.; Westphal, U. H.; Worm, K.; Braslavsky, S. E.; Schaffner, K. *J. Photochem. Photobiol. B* **1996**, *34*, 73. (b) Kneip, K., Mozley, D., Hildebrandt, P.; Gärtner, W.; Braslavsky, S. E.; Schaffner, K. *FEBS Lett.* **1997**, *414*, 23.
(34) Cox, P. J.; Parker, S. F. *Acta Crystallogr.* **1996**, *C52*, 2578.
(35) Nygaard, L.; Nielsen, J. T.; Kirchheiner, J.; Maltesen, G.; Rastrup-Andersen, J.; Sørensen, G. O. *J. Mol. Struct.* **1969**, *3*, 491.
(36) Christen, D.; Griffiths, J. H.; Sheridan, J. *Z. Naturforsch.* **1981**, *36a*, 1378.
(37) Nygaard, L.; Christen, D.; Nielsen, J. T.; Pedersen, E. J.; Snerling, O.; Vestergaard, E.; Sørensen, G. O. *J. Mol. Struct.* **1974**, *22*, 401.
(38) Eng-Wilmot, D. L.; van der Helm, D. *J. Am. Chem. Soc.* **1980**, *102*, 7719.
(39) (a) Kuchitsu, K. In *Accurate Molecular Structures*; Domenicano, A., Hargittai, I., Eds.; Oxford University Press: Oxford, 1992; p. 14. (b) Hargittai, M.; Hargittai, I. *Int. J. Quantum Chem.* **1992**, *44*, 1057.
(40) Lide, D. R., Jr. *J. Chem. Phys.* **1960**, *33*, 1514.
(41) The mean or average deviations are defined by the root-mean-square (rms) error; the expresssions will be used indiscriminately.
(42) Harsányi, L.; Vajda, E.; Hargittai, I. *J. Mol. Struct.* **1985**, *129*, 315.
(43) (a) Ferenczy, G.; Harsányi, L.; Rozsondai, B.; Hargittai, I. *J. Mol. Struct.* **1986**, *140*, 71. (b) data as cited in Harsányi, L.; Császár, P.; Császár,A. *Int. J. Quantum Chem.* **1986**, *29*, 799.
(44) O'Gorman, J. M.; Shand, W., Jr.; Schomaker, V. *J. Am. Chem. Soc.* **1950**, *72*, 4222.
(45) Pyckhout, W.; van Alsenoy, C.; Geise, H. J. *J. Mol. Struct.* **1986**, *144*, 265.
(46) Kuchitsu, K.; Fukuyama, T.; Morino, Y. *J. Mol. Struct.* **1967/68**, *1*, 463.
(47) Kuchitsu, K. *J. Chem. Phys.* **1968**, *49*, 4456.
(48) Simandiras, E. D.; Handy, N. C.; Amos, R. D. *J. Phys. Chem.* **1988**, *92*, 1739.
(49) Pulay, P.; Fogarasi, G.; Pang, F.; Boggs, J. E. *J. Am. Chem. Soc.* **1979**, *101*, 2550.
(50) Smit, K. Ph.D. Thesis, Universität Duisburg, 1992.
(51) Baker, J.; Jarzecki, A. A.; Pulay, P. *J. Phys. Chem.* **1998**, *A102*, 1412.
(52) Goodman, L.; Ozkabak, A. G.; Thakur, S. N. *J. Phys. Chem.* **1991**, *95*, 9044.
(53) Snavely, D. L.; Blackburn, F. R.; Ranasinghe, Y.; Walters, V. A.; Gonzalez del Riego, M. *J. Phys. Chem.* **1992**, *96*, 3599.
(54) Mizugai, Y.; Katayama, M. *Chem. Phys. Lett.* **1980**, *73*, 240.
(55) Foldes, A.; Sandorfy, C. *Can. J. Chem.* **1970**, *48*, 2197.
(56) (a) Navarro, R.; Orza, J. M. *An. Quím.* **1983**, *79*, 557. (b) Navarro, R.; Orza, J. M. *An. Quím.* **1983**, *79*, 571. (c) Navarro, R.; Orza, J. M. *An. Quím.* **1984**, *80*, 59. (d) Navarro, R.; Orza, J. M. *An. Quím.* **1985**, *81*, 5.
(57) Klots, T. D.; Chirico, R. D.; Steele, W. V. *Spectrochim. Acta* **1994**, *50A*, 765.
(58) Majoube, M. *J. Raman Spectrosc.* **1989**, *20*, 49.
(59) Majoube, M.; Vergoten, G. *J. Mol. Struct.* **1992**, *266*, 345.
(60) Woldbaek, T.; Klaboe, P.; Nielsen, C. J. *J. Mol. Struct.* **1975**, *27*, 283.
(61) (a) Barnes, A. J.; Le Gall, L.; Madec, C.; Lauransan, J. *J. Mol. Strcut.* **1977**, *38*, 109. (b) Le Gall, L.; Barnes, A. J. *Ber. Bunsen-Ges. Phys. Chem.* **1978**, *82*, 52.
(62) Giorgini, M. G.; Fortunato, B.; Mirone, P. *Atti. Soc. Nat. Modena* **1975**, *106*, 89.
(63) Ivanov, A. Y.; Plokhotnichenko, A. M.; Radchenko, E. D.; Sheina, G. G.; Blagoi, Y. P. *J. Mol. Struct.* **1995**, *372*, 91.
(64) Barnes, A. J.; Stuckey, M. A.; Le Gall, L. *Spectrochim. Acta* **1984**, *40A*, 419.
(65) Tabacik, V., Pellegrin, V.; Günthard, H. H. *Spectrochim. Acta* **1979**, *35A*, 1055.
(66) Del Bene, J. E.; Person, W. B.; Szczepaniak, K. *J. Phys. Chem.* **1995**, *99*, 10705.
(67) Bock, C. W.; Panchenko, Y. N.; Krasnoshchiokov, S. V.; Pupyshev, V. I. *J. Mol. Struct.* **1985**, *129*, 57.
(68) Wiberg, K. B.; Rosenberg, R. E. *J. Am. Chem. Soc.* **1990**, *112*, 1509.
(69) Furukawa, Y.; Takeuchi, H.; Harada, I.; Tasumi, M. *Bull. Chem. Soc. Jpn.* **1983**, *56*, 392.
(70) Huber-Wälchli, P.; Günthard, Hs. H. *Spectrochim. Acta* **1981**, *37A*, 285.
(71) De Maré, G. R.; Panchenko, Y. N.; Auwera, J. V. *J. Phys. Chem.* **1997**, *A101*, 3998.
(72) Guo, H.; Karplus, M. *J. Chem. Phys.* **1991**, *94*, 3679.
(73) Lee, J. Y.; Hahn, O.; Lee, S. J.; Choi, H. S.; Shim, H.; Mhin, B. J.; Kim, K. S. *J. Phys. Chem.* **1995**, *99*, 1913.
(74) Tang, W.; Bally, T. *J. Phys. Chem.* **1993**, *97*, 4365.
(75) Orza, J. M.; Escribano, R.; Navarro, R. *J. Chem. Soc., Faraday Trans. 2* **1985**, *81*, 653.
(76) Kratky, C.; Falk, H.; Grubmayr, K.; Zrunek, U. *Mh. Chemie* **1985**, *116*, 761.
(77) Polavarapu, P. L. *J. Phys. Chem.* **1990**, *94*, 8106.
(78) Komornicki, A.; McIver, J. W., Jr. *J. Chem. Phys.* **1979**, *70*, 2014.
(79) Panchenko, Y. N. *Spectrochim. Acta* **1975**, *31A*, 1201.
(80) Schrader, B., Meier, W., Eds. *Raman/IR Atlas organischer Verbindungen*; Verlag Chemie: Weinheim, 1974.
(81) Buckingham, A. D.; Harris, B.; LeFèvre, R. J. W. *J. Chem. Soc.* **1953**, 1626.
(82) Miller, M. D.; Jensen, F.; Chapman, O. L.; Houk, K. N. *J. Phys. Chem.* **1989**, *93*, 4495.
(83) Stirling, A. *J. Chem. Phys.* **1996**, *104*, 1254.
(84) (a) Lagant, P.; Derremaux, P.; Vergoten, G.; Peticolas, W. L. *J. Comput. Chem.* **1991**, *12*, 731. (b) Peticolas, W. L.; Strommen, D. P.; Lakshminarayanan, V. *J. Chem. Phys.* **1980**, *73*, 4185. (c) Blazej, D. C.; Peticolas, W. L. *Proc. Natl. Acad. Sci. U.S.A.* **1977**, *74*, 2639.
(85) Morse, P. M. *Phys. Rev.* **1929**, *34*, 57.
(86) Pauling, L.; Wilson, E. B. *Introduction to Quantum Mechanics*; McGraw-Hill: New York, 1935; p 271.
(87) Abramowitz, M.; Stegun, I. A. *Handbook of Mathematical Functions*; 5th ed.; Dover Publications: New York, 1969; eqs 25.3.23 and 25.3.27
(88) van Duijneveldt-van de Rijdt, J. G. C. M.; van Duijneveldt, F. B. *J. Mol. Struct.* **1976**, *35*, 263.
(89) Equation 25.3.24 in ref 87.
(90) Kurtz, H. A.; Stewart, J. J. P.; Dieter, K. M. *J. Comput. Chem.* **1990**, *11*, 82.